EXCITATION TRANSFER IN A QUANTUM SPIN MODEL FOR THE PHOTOSYNTHESIS PROCESS

RAFFAELE CARLONE, ILENIA DI GIORGIO, AND CLAUDIA NEGULESCU

Abstract. Biological processes reveal abilities which are very impressive and cannot be adequately explained with the only use of traditional (classical) approaches. A certain amount of quantum mechanics is thought to be used by nature in order to enhance the efficiency of the underlying processes. The question which arises then is: *How can quantum features survive in an open quantum system subject to a permanent environmental noise*? In this paper we shall present a mathematical model for the illustration of the excitation energy transfer in photosynthesis complexes, with the aim to study the "constructive" interplay between the coherent quantum excitation transfer and the vibrational classical motion of the underlying molecular structure. The model is based on the Schrödinger equation associated to a time-dependent Hamiltonian, describing the propagation of an absorbed photon through a spin-chain towards the reaction center of the photosynthesis apparatus (Spin-Boson model).

Keywords: Quantum mechanics, excitation energy transfer in photosynthesis complexes, Schrödinger equation, spin-boson model, system-environment entanglement, vibrational molecular structure, numerical simulation.

1. Background and motivation

Classical physics seems to be not satisfactory to explain some life processes in living systems which are very performant, letting their technical counterparts far behind and rendering thus humans desirous. To give only some examples, it is for the moment not at all understood how our brain, constituted of a dense network of neurons, is able to deal with such an incredibly large amount of information and what is more, even on very short time scales. Vision and olfaction are other examples of biological processes for which traditional (classical) approaches give no satisfactory answer for explaining their efficient functioning. There are indeed several processes in biological organisms for which it is thought that quantum coherence is used by nature in order to enhance the efficiency of the underlying evolution, see for example [17, 19, 21]. However quantum mechanics requires an isolated framework, and in contrast to classical systems, it is very difficult to protect a quantum system from external noise [5, 18, 24]. Furthermore, quantum features are very sensitive to perturbations, fact which makes the implementation of quantum technology so complicated. Thus the essential question which arises spontaneously is: *How does nature maintain quantum features in an open quantum system, which is in permanent contact*

Date: November 7, 2025.

with a noisy environment? In this sense, the aim of the present paper is to go a step further in the understanding of the performances of a fundamental biological process, namely the excitation energy transfer in photosynthesis complexes. Some evidence of quantum coherence in the photosynthesis process can be found in [13, 20, 25, 26]. This paper is the follow-up of a first work by one of the authors [23] and it is based on the Schrödinger equation (spin-boson model), describing the propagation of an absorbed photon along a spin-chain (representing the chlorophyll molecule-chain) embedded in a vibrational environment. The focus is on the influence of the classical vibrational motion (thermal motion) of the molecular (chlorophyll) structure on the quantum coherent excitation transfer.

1.1. **Open quantum systems and aim of this paper.** The dynamics of open quantum systems has captivated the attention of several researchers in the last years, due to essential applications in quantum computing [6], quantum thermodynamics [22] and quantum biology [1]. The center of activity is the understanding of the effect of the surrounding environment on the central, open quantum system, and the design of simple mathematical models permitting to describe solely the dynamics of interest, namely the one of the central quantum system. Two approaches are mainly considered:

(a) the **fully quantum approach**, which is the most general and precise description, based on the whole "system + environment" modelling. In order to render the system more tractable, in particular to describe only the central system dynamics, one makes use of the reduced density matrix formalism, taking the partial trace of the full density matrix over the environment, eliminating thus the environmental degrees of freedom and leading to the so-called master equation of the central quantum system. This type of asymptotic reduction is mathematically very rigorous.

(b) the **hybrid, quantum-classical approach**, which is an approximate theory, based on a classical description of the (macroscopic) environment. The central system is supposed to evolve via a Schrödinger equation, but governed this time by a time-dependent Hamiltonian, depending on external parameters or stochastic fields, which describe the interaction with the environment. The statistical properties of the stochastic fields determine the properties of the environment and have to be carefully chosen. This type of approach is empirical.

Due to the complex structure of realistic environments and of the environment-system interactions, it is rather hard to obtain in a rigorous mathematical manner a master equation (approach (a)). Most of the time, the description of open quantum systems relies on approximations (approach (b)), which are often mathematically not-justified and may lead to erroneous conclusions. The two approaches presented above differ in the way the environment is modelled, namely as a quantum or a classical bath. At high temperatures, the picture of a classical environment (stochastic noise) is a valid description of the environment. However at low temperatures, the vibrational bath cannot be described any more by an external random, classical field, and requires a full quantum-mechanical description, taking into account for the back-action of the central system on the environment. For more details about these approaches and their limitations see [12, 15] and references therein. A quantitative comparison between the influence of classical and quantum environments on

small quantum systems can be found in [11].

Open questions which are for the moment at the heart of the modelling of open quantum systems are: how to model open quantum systems in a precise and also mathematical tractable manner; how to identify clear signatures of quantum phenomena; is it possible for this to consider the hybrid approach (b) or is the fully quantum approach (a) necessary; is it finally possible to show that quantum systems have clear advantages over their classical counterparts *etc.* The goal of such studies is among others to identify clearly if quantum features are really responsible for an enhancement of biological processes. The present paper tries to give some answers in this direction.

The toy model of this paper is the excitation energy transfer in photosynthesis complexes. The aim is to model mathematically and study numerically how (or if) the interaction with a vibrational environment (heat bath) permits to enhance the transfer of a photon from one end to the other end of a spin-chain, which represents the chlorophyll molecules in a plant leaf. The former paper [23] was based on a fully quantum mechanical approach, and was kept simple in order to be able to do some numerics (only one common environmental bath). However, the model was finally too simple to clearly separate quantum and classical features in the excitation energy transfer. The present paper focus rather on a hybrid quantum-classical approach. The particular question in this paper is to understand the role of the deterministic vibrations of the underlying molecular structure on the quantum-coherent propagation of the excitation through the spin-chain. This is in contrast to a stochastic disturbance by the environment.

This paper is organized as follows. In Section 2 we present the fundamental Spin-Boson model for the description of the excitation transfer in a spin-chain as well as the driven excitation transfer model, where the transfer is guided by the vibrations of the underlying molecular structure. Section 3 is concerned with the analytic computations in the case of a chain consisting of $N = 2$ molecules, permitting to understand the cooperation between the deterministic vibrational motion and the quantum excitation transfer. For longer chains ($N = 7$ in our case) analytical solutions are no more available and numerical simulations are presented and analysed. The paper ends with some conclusions and prospectives.

1.2. **Applications of the Spin-Boson model.** Before going on, let us mention that efficient transfer of (quantum) excitation/energy is essential in various fields of application, ranging from molecular technology, quantum biology to quantum heat-engines. The prototype mathematical model for the description of such transfer phenomena is the Spin-Boson model we shall introduce in subsection 2.1. To understand its extent, let us say some words about three main applications.

Excitation energy transfer in the photosynthesis process [4]:
Photosynthesis is one of the most important biological process on Earth, notably the basis of life on Earth, permitting to capture the abundant sun's energy and to transform it

into chemical energy. In particular chlorophyll-containing plants, algae and cyanobacteria capture via their leafs a broad spectrum of the energy of the sun, transfer the absorbed photons (excitation transfer through a network of pigments) towards a reaction centre, where these are used to enable the photosynthesis reaction to take place, namely

$$6\,CO_2 + 6\,H_2O \rightarrow^{photons} 6\,O_2 + C_6H_{12}O_6\,, \qquad \Delta G = 2.87 * 10^3\ kJ/mol\,.$$

The sun's energy is thus transformed into a chemical energy, stored in the carbohydrate molecule, necessary for the growth of the plant (see Fig 1).

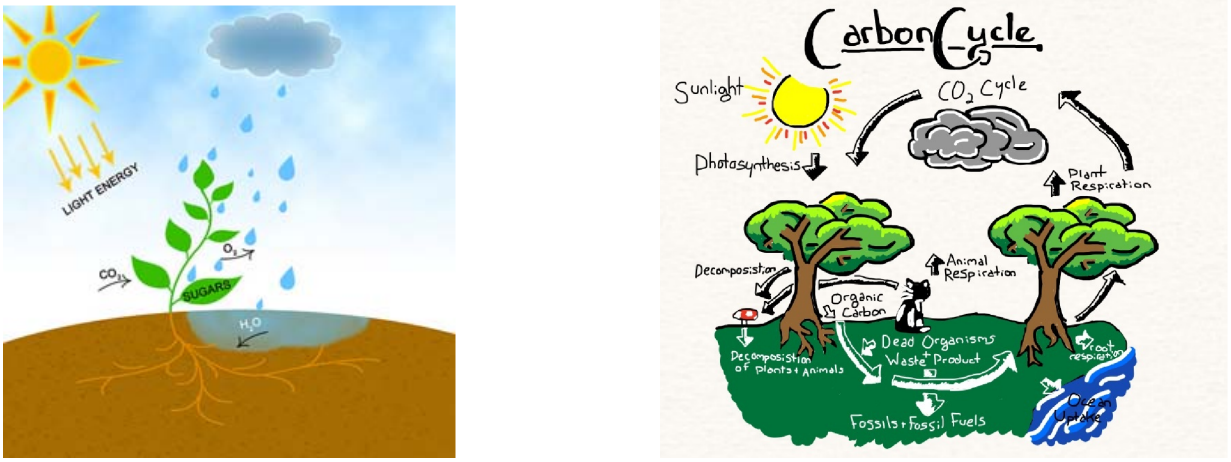

FIGURE 1. The photosynthesis process in plants on the left [https://study.com] and the carbon cycle on the right [https://quizizz.com].

Biological systems are very complex, in particular the photosynthesis process involves many distinctive stages. In this paper we are only interested in the modelling and the understanding of the efficient excitation energy transfer, from the absorption of the photons to their delivery to the reaction center. This energy transfer in plants is remarkably efficient, in the sense that the probability of an absorbed photon, to contribute to the charge-separation in the reaction center, is nearly 100%. A better comprehension of this perfect efficiency would be a very important step in the domain of *information processing*.

Signal transfer in neural networks [10]:
Other biological processes seem to exploit the role of the environmental noise in order to enhance the excitation transfer. Indeed, there are certain aspects in the activity of the brain that appear to have no obvious explanation based on traditional, classical neuroscience. For example all proposed biological memory models lack to explain the obvious correlations between distant neurons, which fire simultaneously. Furthermore, classical approaches are deficient in explaining the phenomenal speed with which our brain processes the information. Modelling the brain as a quantum system could allow to understand better some of these problems.

Neurons (cells within the nervous system) are the basic working unit of the brain, and are constituted of a cell-body (soma), dentrities which are cellular extension able to receive signals (electrochemical stimulations) coming from neighbouring neurons, and an axon, which transmits a signal across the so-called synapses towards the other neurons (see Fig. 2). The human brain consists approximately of 10^{11} nerve cells. They are organized in a dense network, and are designed to receive and transmit information to other nerve cells. One of the unique features of nerve cells is their capability to communicate with each other with great precision, even if they are separated by long distances. The basic ingredients of a neuronal network are:

- the processing element (neuron);
- the inter-connection structures between neurons;
- the network dynamics;
- the learning rules which govern the modification of the inter-connection strengths.

The simplest caricature of a neuron is a two-level system, with two states, namely

- the ground state (neuron is at rest);
- the excited state (neuron fires).

Each neuron plays the role of a switch whose connections (synapses) to other neurons are weighted according to its past experience (learning).

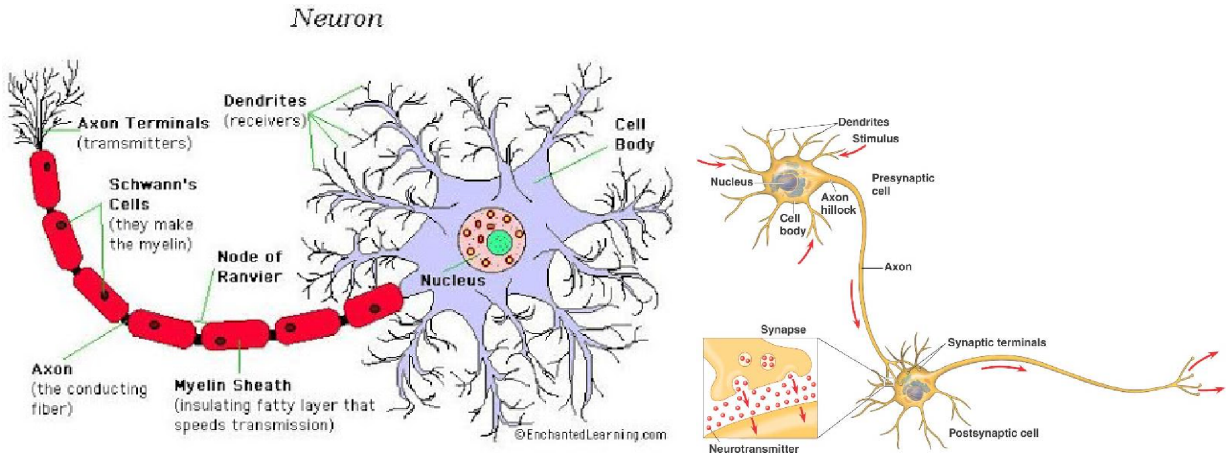

FIGURE 2. The axon (https://www.enchantedlearning.com) and the signal transfer through the nervous system (https://socratic.org)

The Spin-Boson model introduced in Section 2.1 can be used to describe the firing in a simplified neuronal network and the ensuing decoherence due to interaction with the surrounding environment. The property of non-locality (correlations between distant molecules) observed also in the excitation energy transfer of photosynthesis systems may be one of the fundamental properties permitting to explain the exceptional speed with which our brain treats informations.

Information transfer via spin chains [3, 14]:
Classical communications run through constructions such as radio channels, optical fibers or cooper wires, which transfer the processing element (classical bit) in form of electromagnetic waves or optical pulses. On very small scales however (quantum scales), one needs a new concept to transfer the quantum bit in an effective way.

For the operation of a quantum computer it is fundamental to communicate efficiently between the different components of the computer, such as quantum processors, memories *etc*. This communication is essential not only to transfer information from one point to another, but also to generate entangled states of spatially distant particles (specificity of a quantum computer). From this necessity to communicate emerged the concept of "quantum channel" and a promising class of systems which can serve as reliable quantum channels are spin chains. These chains are defined as a collection of interacting two-level systems (spins) on a graph (see Fig. 3), whose dynamics is governed by an appropriate Hamiltonian. The Spin-Boson model we shall present in the next section is at the basis of this issue.

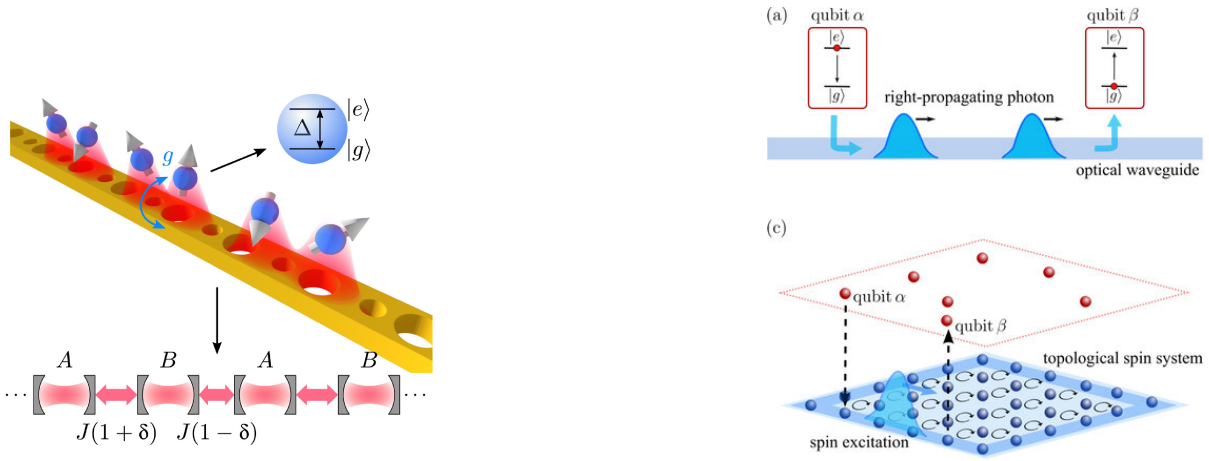

FIGURE 3. Information transfer through quantum channels composed of TLS.

2. The Spin-Boson model and the vibrational driven model

The Spin-Boson model is one of the fundamental models in the description of the interactions of an open quantum system (constituted of two-level systems - TLS) with its bosonic environment. Apart from providing a comprehensive and tractable description of fundamental phenomena, such as quantum entanglement, decoherence *etc*, it finds applications in a wide range of topics, as mentioned in the introduction. Let us thus introduce this model briefly in the next subsection and refer the reader interested in more details to the work [24].

2.1. **Presentation of the full quantum model.**

Let us consider a simple version of the Spin-Boson model, consisting of a chain of N coupled two-level systems (1/2-spins)

interacting with a bath of harmonic oscillators (K bosonic modes). The dynamics of this open quantum system is governed by the Schrödinger equation

$$\mathbf{i}\hbar\,\partial_t\psi = H\,\psi\,, \tag{1}$$

where the quantum state is completely described by the wavefunction $\psi(t)$ in the Hilbert-space $\mathcal{H} = \mathbb{C}^{2N} \otimes \mathcal{F}$ where $\mathcal{F}$ is a boson Fock space. The Hamiltonian of the whole system consists of three components, corresponding to the dynamics of the central spin-chain ($\mathcal{S}$), the vibrational bosonic environment ($\mathcal{E}$) as well as the interaction between these two subsystems ($\mathcal{I}$), and writes

$$H = H_{\mathcal{S}} \otimes \mathbb{I}_{\mathcal{F}} + \mathbb{I}_{\mathbb{C}^{2N}} \otimes H_{\mathcal{E}} + H_{\mathcal{I}}\,, \tag{2}$$

with

$$H_{\mathcal{S}} := \frac{\hbar}{2}\sum_{l=1}^{N}\omega_l\sigma_l^z + \sum_{l=1}^{N-1}\lambda_l\,\left(\sigma_l^+\,\sigma_{l+1}^- + \sigma_l^-\,\sigma_{l+1}^+\right)\,,\quad H_{\mathcal{E}} := \hbar\sum_{k=1}^{K}\omega_{ho,k}\,\left(\mathbf{a}_k^\dagger\,\mathbf{a}_k + \frac{1}{2}\,Id\right)\,, \tag{3}$$

and

$$H_{\mathcal{I}} := \frac{\hbar}{2}\sum_{k=1}^{K}\sum_{l=1}^{N}\sigma_l^z\,\left(g_{lk}\,\mathbf{a}_k^\dagger + g_{lk}^*\,\mathbf{a}_k\right)\,.$$

For the definition of these three Hamiltonians, it is useful to index an operator acting only on the l^{th} two-level system by l, as follows

$$\sigma_l^z := \Pi_{i=1}^{l-1}\,\mathbb{I}_i^{\mathbb{C}^2}\otimes\sigma_z\otimes\Pi_{i=l+1}^{N}\,\mathbb{I}_i^{\mathbb{C}^2}\,,\quad \forall l = 1,\cdots,N\,,$$

and for $l < j$ to define

$$\sigma_l^+\,\sigma_j^- := \Pi_{i=1}^{l-1}\,\mathbb{I}_i^{\mathbb{C}^2}\otimes\sigma^+\otimes\Pi_{i=l+1}^{j-1}\,\mathbb{I}_i^{\mathbb{C}^2}\otimes\sigma^-\otimes\Pi_{i=j+1}^{N}\,\mathbb{I}_i^{\mathbb{C}^2}\,, \tag{4}$$

where $\sigma^\pm := \frac{\sigma_x \pm \mathbf{i}\,\sigma_y}{2}$ are the raising (+) resp. lowering (−) operators of the corresponding two-level atoms and $\mathbb{I}_i^{\mathbb{C}^2}$ is the identity operator on $\mathbb{C}^2$. The action of the operator $\sigma_l^+\,\sigma_j^-$ is the raising of the spin at position l and the lowering of the spin at position j. We recall here for completeness the standard complex Pauli matrices σ_x, σ_y and σ_z, given by

$$\sigma_x = \begin{pmatrix} 0 & 1 \\ 1 & 0 \end{pmatrix}\,,\quad \sigma_y = \begin{pmatrix} 0 & -\mathbf{i} \\ \mathbf{i} & 0 \end{pmatrix}\,,\quad \sigma_z = \begin{pmatrix} 1 & 0 \\ 0 & -1 \end{pmatrix}\,.$$

Furthermore, we denote by λ_l the strength of the interaction (of dipole-dipole type) between two neighbouring TLS, by $\hbar\,\omega_l$ the transition energy between ground and excited state of the l^{th} TLS and by ω_{ho} the quantum harmonic oscillator's frequency, where $\mathbf{a}$ resp. $\mathbf{a}^\dagger$ are the so-called phonon annihilation resp. creation operators. Finally g_l is the interaction strength between the TLS and the bath. As explained in [23] we shall restrict this study to the single-excitation subspace and shall also assume that the molecules are sufficiently distant from each other, so that their mutual dipole-interactions can be reduced to the dominant interaction between neighbouring molecules.

For a more detailed explanation of this fully quantum model, we refer the interested reader to the first part of this work [23], where it was used to study the influence of a bath-environment on the excitation transfer. The distinctive feature of this dephasing model, is that there is no relaxation between the spin-chain and the environment. Indeed, due to $[H_{\mathcal{I}}, \sigma_z] = 0$ which yields $[H_{\mathcal{I}}, H_{\mathcal{S}}] = 0$, the excitation is conserved, such that decoherence is induced here by dephasing only, a situation where we deal with entropy-exchange rather than energy-exchange.

2.2. **Different mathematical descriptions.** Different levels of mathematical descriptions are available for the modelling of the dynamics of open quantum system. The three approaches presented below differ in the modelling point of view, complexity and precision. For more details we refer the interested reader to the works [8, 15] and the references therein. In a first work [23] one of the authors focused on a fully quantum model in order to investigate in more details the influence of an environment on the coherent transfer of the excitation, however the model was finally too simple (due to computational reasons) in order to get a conclusive answer. In this second work we focuse rather on a hybrid classical-quantum model, simplifying the environmental modelling by introducing a time-dependence in the Hamiltonian.

The quantum description of the complete "central system + environment" (considered as a single quantum entity) is based on the Schrödinger equation or the equivalent von Neumann equation for pure states

$$\mathbf{i}\hbar\,\partial_t\psi = H_{fq}\,\psi \quad \text{resp.} \quad \mathbf{i}\hbar\,\partial_t\rho = [H_{fq}, \rho]\,, \tag{5}$$

where H_{fq} is the full quantum Hamiltonian given in (2), and where ψ is the wavefunction describing both central system and environment with associated density matrix $\rho := |\psi\rangle\,\langle\psi|$, using the bra-ket notation.

The knowledge of the dynamics of the environment is not so meaningful, essential is rather its influence on the central system. To render the numerical computations more tractable, one can then reduce the problem by tracing out the environment, and considering only the central system dynamics. This average over the environmental degrees of freedom leads to the problem

$$\mathbf{i}\hbar\,\partial_t\rho_{\mathcal{S}} = tr_{\mathcal{E}}\,[H_{fq}, \rho]\,, \qquad \rho_{\mathcal{S}} = tr_{\mathcal{E}}(\rho)\,.$$

Remark that this system is not closed. Different approximations and simplifications (for ex. the Born-approximation) permit to close the system and yield a so-called master equation

$$\mathbf{i}\hbar\,\partial_t\rho_{qua} = \mathcal{L}\,\rho_{qua}\,, \tag{6}$$

with $\mathcal{L}$ an operator (called sometimes super-operator) which incorporates the effects of the environment. The master equation gives the evolution of an open quantum system, replacing the von Neumann equation (5) for isolated systems. To draw a parallel with classical mechanics, this passage from a microscopic (reversible) world to a more macroscopic (irreversible) level of description (separating time-scales and averaging) is similar to the

passage "Newton's equation" $\mapsto$ "Boltzmann's equation" in classical statistical mechanics.

More often than one may think, the irreversible dynamics of the open quantum system may be modelled entirely without invoking a quantum environment. The dynamics turns out to be (sometimes!) indistinguishable from a random unitary evolution, which can be thought of as arising from classical random fluctuations. This mixed "quantum-classical" approach describes the dynamics of the open central system under the influence of an external environment via the following von Neumann equation (for mixed states)

$$\mathbf{i}\hbar\,\partial_t\rho_{qc} = [H_{qc}, \rho_{qc}]\,, \qquad H_{qc} := H_{\mathcal{S}} + H_{pert}\,, \qquad H_{pert} = \frac{\hbar}{2}\sum_{l=1}^{N}\eta_l(t)\sigma_l^z\,, \tag{7}$$

where $H_{\mathcal{S}}$ is the standard central system Hamiltonian (2) and H_{pert} is the perturbation Hamiltonian. This last one represents the influence of an external, macroscopic and classical environment on the central system, via some random classical source of noise, such as stochastic Gaussian fields $\eta_l(t)$. This mixed quantum-classical equation has to be compared with the resembling quantum master equation (6). To demonstrate the quantum $\leftrightarrow$ mixed quantum-classical equivalence (if any), one has to be able to find an adequate perturbation Hamiltonian (or equivalently adequate stochastic fields $\eta_l(t)$), such that $\rho_{qua}(t) = \rho_{qc}(t)$ for all times. This is not so evident and not all quantum models have a classical analogue. If one would find such an equivalence, this would mean that while the evolution of isolated quantum systems is fully deterministic, open quantum systems are stochastic in nature. The effect of a dephasing environment on the system of interest would then consist in solely introducing stochastic perturbations in the eigenvalues of the central system.

Finally, a complete classical description of the problem can be written under the form of Liouville's equation

$$\partial_t\rho_{cl} = \{H_{cl}, \rho_{cl}\}\,, \qquad \{f, g\} := \partial_x f\,\partial_p g - \partial_p f\,\partial_x g\,, \tag{8}$$

with $H_{cl}(x, p)$ the classical Hamiltonian, $\{\cdot,\cdot\}$ the Poisson bracket and $\rho_{cl}(x, p)$ the phase-space density matrix corresponding to the classical system.

2.3. **A driven excitation energy transfer model.** The present paper is based on a hybrid quantum-classical model for describing the quantum excitation energy transfer (EET) in a spin-chain (photosynthesis complex), where the spins undergo classical mechanical oscillations, corresponding to the thermal vibrations of the underlying molecular structure. One important point to be investigated is the question if an ingenious choice of the underlying mechanical motion (external frequency) can enhance the EET.

Before introducing the time-dependent model, let us recall the *single-excitation framework* used throughout this work. The full Hilbert space of the spin chain is $\mathcal{H} = (\mathbb{C}^2)^{\otimes N}$, of total dimension 2^N, corresponding to all possible spin configurations. However, since

the Hamiltonian (3) commutes with the total excitation-number operator

$$\hat{N} = \sum_{l=1}^{N} \frac{\sigma_l^z + I}{2},$$

the total number of excitations is conserved during the evolution. Consequently, $\mathcal{H}$ decomposes into invariant subspaces labeled by the number of excitations. In this work we restrict to the *single-excitation subspace* $\mathcal{H}_1$, spanned by the orthonormal basis $\{|e_l\rangle\}_{l=1}^N$, where $|e_l\rangle$ denotes the configuration in which only the l-th spin is in the excited state while all the others remain in their ground state:

$$|e_l\rangle = |--\cdots-+\cdots-\rangle.$$

Within this subspace, the quantum state of the system can be written as

$$|\Psi(t)\rangle = \sum_{l=1}^{N} \psi_l(t)|e_l\rangle,$$

so that the wavefunction can be represented as an N-component spinor wave-vector $\Psi(t) = (\psi_1(t), \ldots, \psi_N(t))^T \in \mathbb{C}^N$. The effective Hamiltonian acting on this reduced state vector is then an $N \times N$ matrix, whose entries are determined by the coupling coefficients $\lambda_l(t)$ between neighbouring sites. This reduction is fully justified because, starting from a single initial excitation, the entire dynamics remains confined within the subspace $\mathcal{H}_1$.

Given this framework, we can now introduce the driven model, which describes how the excitation propagates along the spin-chain when the molecular sites are subject to classical vibrations. Let us start with the model presented in subsection 2.1, however we shall not consider the interaction of our spin-chain with a random, noisy, dephasing environment. Instead we shall rather concentrate on the coherent excitation energy transfer in a spin-chain embedded in a *vibrational classical environment*, whose effect is to introduce an oscillatory motion of the molecules constituting the spin-chain (see Fig. 4). Hence, the dynamics of the wavefunction Ψ is governed by Schrödinger's equation

$$\mathbf{i}\hbar\, \partial_t \Psi(t) = H_{\mathcal{S}}(t)\, \Psi(t)\,, \qquad \forall t > 0\,, \tag{9}$$

where $H_{\mathcal{S}}(t)$ is of the form (3), however with time-dependent coupling coefficients $\lambda_l(t)$. We shall start at instant $t = 0$ from the configuration of an absorbed excitation by the first two-level system, whereas all other spins are in the ground state. As already mentioned, in the single-excitation framework the participating configurations are regrouped in a spinor wave-function

$$\Psi \in \mathbb{C}^N\,, \qquad \Psi(t) := (\psi_l(t))_{l=1}^N\,, \qquad \psi_l(t) = \psi_{--\cdots-+-\cdots-}\,,$$

where the + sign represents the excited state and the wave-function $\psi_l(t)$ corresponds to the configuration with the excitation localized at the l^{th} atom.

In [23] we considered constant (in time) transition energies ω_l as well as constant coupling coefficients λ_l. The vibrational motion of the underlying molecular structure induces

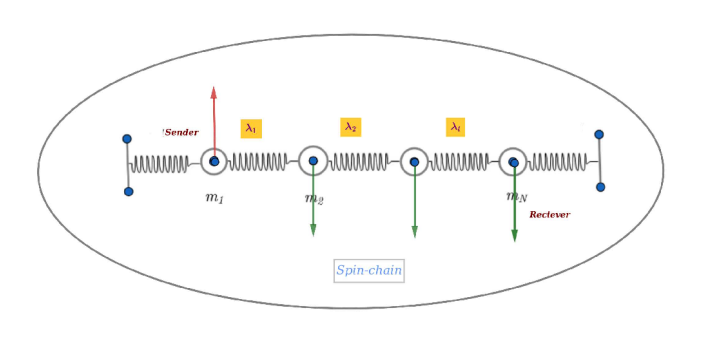

FIGURE 4. Sketch of the considered spin-chain, embedded in an exteriour vibrational environment. The first TLS is initially excited, and this excitation is then transferred towards the receiver.

however a time-dependence of these coefficients and hence a time-dependent Hamiltonian $H_{\mathcal{S}}(t)$. Indeed, the vibrations of the molecules change the relative distances between the two-level systems, and thus the distance-dependent dipole couplings λ_l. At the same time, the small changes in the positions of the molecules can also induce a modulation of the transition energies ω_l, due to the fact that these two-level systems can be immersed in a space-dependent magnetic field $\mathbf{B}(x)$. This last point will be however not considered here.

Denoting by $z_l(t)$ the displacements of the molecules with respect to their equilibrium positions, the distance between the l^{th} and the $(l+1)^{th}$ spin is given by

$$d_l(t) := d_0 - [z_l(t) - z_{l+1}(t)] \,, \qquad \forall t > 0 \,, \quad l = 1, \cdots, N-1 \,,$$

where $d_0 > 0$ is the constant equilibrium distance between the spins. For example a driven, simple sinusoidal motion, with vibrational frequency $\omega_v > 0$, is described by

$$d_l(t) := d_0 \, [1 - 2a_l \, \sin(\omega_v \, t + \varphi_l)] \,, \qquad \forall t > 0 \,, \quad l = 1, \cdots, N-1 \,, \tag{10}$$

with a_l the amplitude and φ_l the phase of the individual sites. A different driving motion, mainly used in engineering applications, is given under the form of a Gaussian wave-packet

$$d_l(t) := d_0 \left[1 - a \, e^{-\frac{[(l-1)d_0 - vt]^2}{2\,\sigma^2}} \right] \,, \qquad \forall t > 0 \,, \quad l = 1, \cdots, N-1 \,,$$

with $\sigma > 0$ the pulse width, $a > 0$ the amplitude and v the velocity of the wave-packet. This motion corresponds to an exteriour guiding of the underlying molecular displacements, under the form of a pulse which propagates along the spin-chain, with its center at the position $ld_0 = vt + d_0$. The effect of the pulse is to concentrate the molecules in a certain region of the chain (which moves) and thus to couple more strongly these molecules, whereas the coupling of the rest part of the chain remains unaffected. This type of external guiding shall however not be treated in this paper, we shall rather focus on the oscillatory motion (10).

The coupling strengths $\lambda_l(t)$ are now imposed by the distances between the neighbouring spins, via the formula (dipole-dipole interactions)

$$\lambda_l(t) := \frac{\tilde{\lambda}_l}{\left[d_l(t)/d_0\right]^3}\,, \qquad \forall t > 0\,, \quad l = 1, \cdots, N-1\,, \tag{11}$$

where $\tilde{\lambda}_l$ are the time-independent couplings of the molecular static chain. This formula underlines the fact that the closer the TLSs are, the stronger the coupling is.

Given all these coefficients, one can solve the Schrödinger equation (9) and compute now the **site occupation probabilities** $\mathcal{P}_l(t)$ of the l^{th} two-level system via

$$\mathcal{P}_l(t) := |\psi_l(t)|^2\,, \quad \forall l = 1, \cdots, N\,, \tag{12}$$

quantities which shall permit to localize the excitation in the spin-chain, and thus to study the excitation transfer from one end-point to the other of the spin-chain. These probability functions depend naturally on $\{\lambda_l(t)\}_{l=1}^{N-1}$ and hence on the external mechanical frequency ω_v. Thus, an effective interplay between the mechanical oscillations (ω_v) on one hand, and the eigen-frequencies of the non-perturbed spin-chain (ω_l for $l = 1, \cdots, N$) on the other hand, could improve the excitation energy transfer. Our aim is to tune the model in such a manner to get a perfect excitation energy transfer in the shortest possible time $t_\sharp$ (*i.e.* $\mathcal{P}_N(t_\sharp) = 1$).

To summarize, the hybrid model presented here is based on a cooperative interplay between the quantum coherent dynamics of the excitation along the spin-chain and the mechanical classical vibration of the underlying molecules. The Hamiltonian governing the quantum excitation motion will acquire a time-dependence, induced by the determinisitic motion of the molecular structure, which is a consequence of the thermal classical environment. This leads necessarily to a driven coherent excitation dynamics (Rabi oscillations), which shall be tuned to get an efficient excitation energy transfer from the first to the last two-level system of the spin-chain.

2.4. **Analytical solutions in some specific situations.** Our aim is now to understand how the information (or excitation) is transferred within the spin chain. As explained in the previous subsection, the model is treated within the *single-excitation framework*, where the total excitation number is conserved. To obtain the dynamics of this excitation, one has to solve the Schrödinger equation (9). Even if this linear equation looks simple, it is in general not possible to obtain analytical solutions when the interaction coeffcients $\{\lambda_l(t)\}_{l=1}^{N-1}$ are time-dependent. There are however situations for which this Schrödinger equation can be solved analytically, situations we shall explicit in this subsection.

For this we decompose the Hamiltonian into the constant, diagonal unperturbed spin-chain part H_0, and the time-depending, hermitian interaction part $H_{int}(t)$, namely

$$H_{\mathcal{S}}(t) := H_0 + H_{int}(t) = \begin{pmatrix} \epsilon_1 & 0 & & 0 \\ 0 & \epsilon_2 & 0 & 0 \\ \vdots & & \ddots & \vdots \\ 0 & 0 & 0 & \epsilon_N \end{pmatrix} + \begin{pmatrix} 0 & \lambda_1(t) & & 0 \\ \lambda_1^*(t) & 0 & \lambda_2(t) & 0 \\ \vdots & & \ddots & \vdots \\ 0 & 0 & \lambda_{N-1}^*(t) & 0 \end{pmatrix},$$

with the eigenstates of H_0 (energy-levels of the different possible configurations in our unperturbed spin-chain) given by

$$\epsilon_l := \frac{\hbar}{2} \sum_{j=1}^{N} s_j^{(l)} \omega_j \,, \qquad \forall l = 1, \cdots, N \,,$$

where $s_j^{(l)} := \pm 1$ is the sign of the j^{th} atom in the l^{th} configuration, namely $+1$ for the excited state and -1 for the ground state. The first Hamiltonian H_0 incorporates the energies of the quantum spin-chain in the absence of spin-interactions. The second Hamiltonian $H_{int}(t)$ describes the interaction of the spin-chain with the vibrational environment. The fact that $H_{int}(t)$ is not diagonal leads to transitions between the different eigenstates of H_0.

Filtering out the diagonal part, the solution of the Schrödinger equation (9) can now be expressed as

$$\Psi(t) = \Sigma_{l=1}^{N} \alpha_l(t) e^{-\mathbf{i}\epsilon_l t/\hbar} \, \mathbf{e}_l \,, \qquad H_0 \, \mathbf{e}_l = \epsilon_l \, \mathbf{e}_l \,, \tag{13}$$

called also *interaction representation* of the wave-function, and where $\{\epsilon_l, \mathbf{e}_l\}_{l=1}^N$ are the eigenvalues resp. eigenvectors of H_0. Inserting Ansatz (13) into (9) permits to get a coupled ODE system for the expansion coefficients $\alpha_l(t)$, namely

$$\begin{pmatrix} \alpha_1'(t) \\ \alpha_2'(t) \\ \vdots \\ \alpha_N'(t) \end{pmatrix} = -\frac{\mathbf{i}}{\hbar} \begin{pmatrix} 0 & \lambda_1(t) e^{-\mathbf{i}(\epsilon_2-\epsilon_1)t/\hbar} & & 0 \\ \lambda_1^*(t) e^{\mathbf{i}(\epsilon_2-\epsilon_1)t/\hbar} & 0 & \lambda_2(t) e^{-\mathbf{i}(\epsilon_3-\epsilon_2)t/\hbar} & 0 \\ \vdots & & \ddots & \vdots \\ 0 & 0 & \lambda_{N-1}^*(t) e^{\mathbf{i}(\epsilon_N-\epsilon_{N-1})t/\hbar} & 0 \end{pmatrix} \begin{pmatrix} \alpha_1(t) \\ \alpha_2(t) \\ \vdots \\ \alpha_N(t) \end{pmatrix}. \tag{14}$$

In the absence of interaction $\lambda_l(t) \equiv 0$ for all $l = 1, \cdots N$, we immediately observe that the coefficients $\alpha_l(t)$ are constant in time, which signifies simply that we are in the situation of a stationary solution, with time-independent occupation probabilities. At this point, the idea is now to try to solve system (14). Unfortunately this apparently very simple ODE system cannot be solved analytically in general, and numerical simulations are the only rescue. Explicit computations can be done however in some specific situations we shall precise now, in order to get a feeling of the phenomenon of driven excitation energy transfer.

For example in the case one considers equal, but time-dependent coupling coefficients $\lambda_l(t) \equiv \lambda(t)$, and uniform local energy-levels $\varepsilon_l = \varepsilon$, the computation of the solutions to the Schrödinger equation (9) is trivial. The eigenvalues resp. eigenvectors of the Hamiltonian $H_{\mathcal{S}}$ are given in this case by

$$E_l(t) := \varepsilon + 2\,\lambda(t)\,\cos\left(\frac{\pi\,l}{N+1}\right)\,, \qquad \phi_l = \sqrt{\frac{2}{N+1}}\,\sum_{j=1}^{N}\sin\left(\frac{\pi\,l\,j}{N+1}\right)\,\mathbf{e}_j\,, \quad l = 1, \cdots, N\,,$$

and the solution to $\mathbf{i}\hbar\,\partial_t\Psi(t) = H_{\mathcal{S}}\Psi(t)$, with initial condition $\Psi(0) = \mathbf{e}_1$, takes the form

$$\Psi(t) = \Sigma_{l=1}^{N}\beta_l\,e^{-\mathbf{i}\mathfrak{E}_l(t)/\hbar}\,\phi_l\,, \quad \beta_l = \sqrt{\frac{2}{N+1}}\,\sin\left(\frac{\pi\,l}{N+1}\right)\,, \quad l = 1, \cdots, N\,, \tag{15}$$

with the primitive of the eigenvalues given for $l = 1, \cdots, N$ by

$$\mathfrak{E}_l(t) = \varepsilon\,t + \mu_l\,\Lambda(t)\,, \qquad \mu_l := 2\,\cos\left(\frac{\pi\,l}{N+1}\right)\,, \quad \Lambda(t) := \int_0^t \lambda(s)\,ds\,.$$

This yields for each component of the wave-function the exact expression

$$\psi_k(t) = \frac{2}{N+1}e^{-\mathbf{i}\,\varepsilon\,t/\hbar}\sum_{l=1}^{N}\sin\left(\frac{\pi l}{N+1}\right)\sin\left(\frac{k\pi l}{N+1}\right)e^{-\mathbf{i}\mu_l\Lambda(t)/\hbar}, \qquad k = 1, \ldots, N\,,$$

and in particular for the last spin-up configuration ($k = N$)

$$\psi_N(t) = -\frac{2}{N+1}\,e^{-\mathbf{i}\,\varepsilon\,t/\hbar}\,\sum_{l=1}^{N}(-1)^l\,\sin^2\left(\frac{\pi\,l}{N+1}\right)\,e^{-\mathbf{i}\mu_l\Lambda(t)/\hbar}\,.$$

The occupation probability of each spin $k = 1, \ldots, N$ is then given by

$$\begin{aligned}\mathcal{P}_k(t) = 2\,\frac{4}{(N+1)^2}\sum_{l=1}^{N}\sum_{h<l}\,\sin\left(\frac{\pi\,l}{N+1}\right)\,\sin\left(\frac{\pi\,k\,l}{N+1}\right)\,\sin\left(\frac{\pi\,h}{N+1}\right)\,\sin\left(\frac{\pi\,h\,k}{N+1}\right)*\\ *\cos\left(\frac{2}{\hbar}\,\Lambda(t)\,\left[\cos\left(\frac{\pi\,l}{N+1}\right) - \cos\left(\frac{\pi\,h}{N+1}\right)\right]\right) + \frac{4}{(N+1)^2}\sum_{l=1}^{N}\sin^2\left(\frac{\pi\,l}{N+1}\right)\,\sin^2\left(\frac{\pi\,k\,l}{N+1}\right)\,,\end{aligned} \tag{16}$$

in particular, one has for the last spin ($k = N$)

$$\begin{aligned}\mathcal{P}_N(t) = 2\,\frac{4}{(N+1)^2}\sum_{l=1}^{N}\sum_{h<l}(-1)^{l+h}\,\sin^2\left(\frac{\pi\,l}{N+1}\right)\,\sin^2\left(\frac{\pi\,h}{N+1}\right)*\\ *\cos\left(\frac{2}{\hbar}\,\Lambda(t)\,\left[\cos\left(\frac{\pi\,l}{N+1}\right) - \cos\left(\frac{\pi\,h}{N+1}\right)\right]\right) + \frac{4}{(N+1)^2}\sum_{l=1}^{N}\sin^4\left(\frac{\pi\,l}{N+1}\right)\,.\end{aligned} \tag{17}$$

What can be observed from these formulae is that the effect of the magnitude of a constant coupling strength λ is nothing but a time-scaling. Furthermore, we can check that the excitation transfer is no more fully achieved for $N > 3$ and constant λ, in particular the probability of the excitation to reach the final spin reduces with the length of the chain,

the reason being the dispersion of the initial excitation over the whole chain (see [9] and Figure 5). For $N = 3$ one can prove the following property.

Lemma 2.1. *If we consider a driven model with three spins ($N = 3$) and equal, positive as well as time-depending coupling coefficients $\lambda(t) > 0$, then there exists a time $t_\sharp > 0$ at which the occupation probability $\mathcal{P}_3(t)$, which reads*

$$\mathcal{P}_3(t) = \sin^4\left(\frac{1}{\sqrt{2}\,\hbar}\Lambda(t)\right), \quad \forall t \geq 0\,,$$

is equal to one, thus we have complete excitation transfer in a finite time.

Proof. Using formula (17) for $N = 3$ one gets

$$\mathcal{P}_3(t) = \frac{1}{4}\cos^2\left(\frac{\sqrt{2}}{\hbar}\Lambda(t)\right) - \frac{1}{2}\cos\left(\frac{\sqrt{2}}{\hbar}\Lambda(t)\right) + \frac{1}{4} = \frac{1}{4}\left[\cos\left(\frac{\sqrt{2}}{\hbar}\Lambda(t)\right) - 1\right]^2, \quad \forall t > 0.$$

Thus

$$\mathcal{P}_3(t_\sharp) = 1 \Longleftrightarrow \cos\left(\frac{\sqrt{2}}{\hbar}\Lambda(t_\sharp)\right) = -1 \Longleftrightarrow \Lambda(t_\sharp) = \frac{(2\,k+1)\,\pi\,\hbar}{\sqrt{2}}, \quad \forall k \in \mathbb{N}\,.$$

As $\Lambda'(t) = \lambda(t) > 0$, the function $\Lambda(t)$ is strictly increasing, starting from $\Lambda(0) = 0$, such that one can find several complete transfer times $t_\sharp^{(k)} := \Lambda^{-1}\left(\frac{(2\,k+1)\,\pi\,\hbar}{\sqrt{2}}\right) > 0$ for each $k \in \mathbb{N}$, for which $\mathcal{P}_3(t_\sharp^{(k)}) = 1$. □

These computations become difficult in the time-dependent general case $(\varepsilon_l, \lambda_l(t))_{l=1}^N$ and we shall turn in subsection 3.2 towards numerical methods.

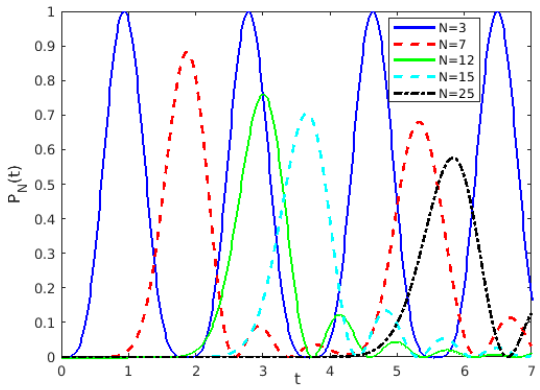

FIGURE 5. Plot of the time-evolution of the occupation probability $\mathcal{P}_N(t)$, for several $N = 3, 7, 12, 15, 25$ and constant coupling strength $\lambda = 2.4$.

3. Study of the vibrational induced enhancement of the excitation transfer

3.1. **Driven model for two spins.** Let us investigate in this subsection a chain constituted of only two spins and examine the occupation probabilities $\{\mathcal{P}_l(t)\}_{l=1}^2$ in order to understand in more details in this simplified framework the influence of the mechanical vibration on the quantum excitation energy transfer. Denoting by $Z(t) := (\alpha_1(t), \alpha_2(t))^{\mathbf{t}}$ the coefficients arising in (13), we have to solve

$$Z'(t) = -\frac{\mathbf{i}}{\hbar}\,\lambda(t)\begin{pmatrix} 0 & e^{-\mathbf{i}\omega_c t} \\ e^{\mathbf{i}\omega_c t} & 0 \end{pmatrix} Z(t)\,, \qquad \omega_c := \frac{\epsilon_2 - \epsilon_1}{\hbar}\,, \tag{18}$$

for an initial condition $Z(0) = (1,0)^{\mathbf{t}}$. The parameter $\omega_c > 0$ represents the transition frequency between the two energy-levels of the system. An explicit solution to (18) can be found only in some specific situations, we shall study now.

3.1.1. *Constant coefficient case: $\lambda > 0$ and $\omega_c \equiv 0$.* In the case of constant coupling coefficients and equal energy levels $\varepsilon_l = \varepsilon$ one can easily compute the occupation probabilities via (17), yielding

$$\mathcal{P}_1(t) = |\psi_1(t)|^2 = \cos^2\left(\frac{\lambda\, t}{\hbar}\right)\,, \qquad \mathcal{P}_2(t) = |\psi_2(t)|^2 = \sin^2\left(\frac{\lambda\, t}{\hbar}\right)\,, \quad \forall t > 0\,.$$

A beating phenomenon is observed, the excitation is transferred regularly forth and back between the first and the second TLS, with an angular frequency of $\omega_R := 2\,\frac{\lambda}{\hbar}$. This phenomenon is known as *Rabbi oscillations* (see left of Fig. 6). Rabi oscillations are a quantum mechanical phenomenon where a two-level system undergoes periodic oscillations between its states when exposed to an exteriour resonant electromagnetic field. Essentially, Rabi phenomenon describes the continuous exchange of energy between the quantum system and the driving field, leading to observable oscillations in the population of the two levels.

Coming back to our spin-chain, we have always in this situation a perfect transfer from site one towards site two, with a transfer time of $t_\sharp = \frac{\hbar\pi}{2\,\lambda}$, which decreases with the increase of the coupling strength. In order to catch the excitation at the end-point of the spin-chain, one has to know exactly when this excitation arrived at destination, this knowledge being crucial for applications.

3.1.2. *Constant coupling $\lambda > 0$, different energy levels $\omega_c \neq 0$.* The situation is different when the energy-levels are not any more equal. In this case, there is no more full excitation transfer. Indeed, one can compute analytically in this case the solution to (18), yielding for all $t > 0$

$$\mathcal{P}_1(t) = \frac{(\lambda/\hbar)^2}{(\lambda/\hbar)^2 + (\omega_c/2)^2}\,\cos^2\left(\frac{\omega_R}{2}\,t\right) + \frac{\omega_c^2}{\omega_R^2}\,, \qquad \mathcal{P}_2(t) = \frac{(\lambda/\hbar)^2}{(\lambda/\hbar)^2 + (\omega_c/2)^2}\,\sin^2\left(\frac{\omega_R}{2}\,t\right)\,, \tag{19}$$

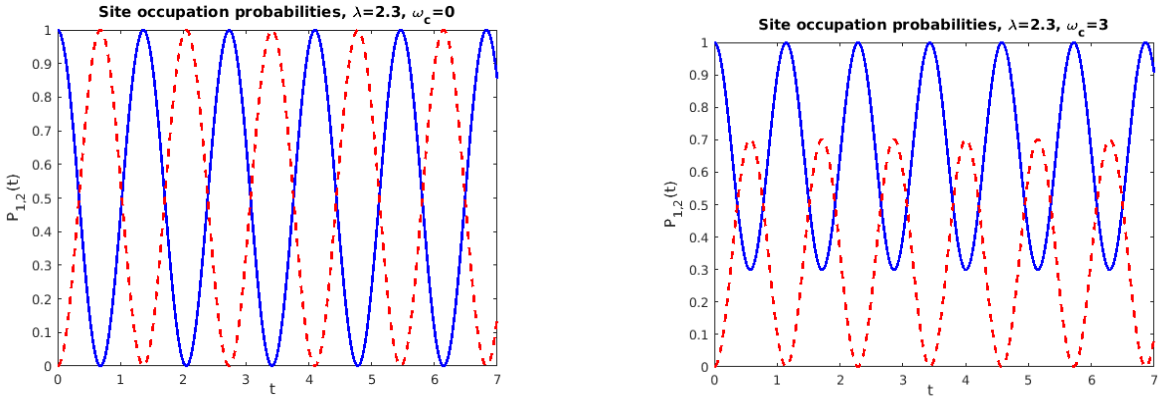

FIGURE 6. Site occupation probability $\mathcal{P}_1(t)$ in blue (full line) resp. $\mathcal{P}_2(t)$ in red (dashed line), for a constant coupling strength $\lambda = 2.3$. Left: $\omega_c = 0$. Right: $\omega_c = 3$.

where ω_R is the so-called (angular) Rabi-frequency, defined as

$$\omega_R^2 := 4\,(\lambda/\hbar)^2 + \omega_c^2\,.$$

One can observe that the excitation oscillates forth and back, with Rabi-frequency ω_R and an amplitude of $\frac{(\lambda/\hbar)^2}{(\lambda/\hbar)^2+(\omega_c/2)^2}$, which never reaches one for $\omega_c \neq 0$. Even if the transfer is not perfect, its transfer time is given by $t_\sharp = \frac{\pi}{\omega_R}$. In the limit of vanishing ω_c or strong coupling strength, meaning for $\hbar\,\omega_c \ll 2\,\lambda$ one gets exactly the previous case

$$\lim_{\frac{\hbar\omega_c}{2\,\lambda}\to 0} \mathcal{P}_2(t) = \sin^2\left(\frac{\lambda\,t}{\hbar}\right)\,, \qquad \lim_{\frac{\hbar\omega_c}{2\,\lambda}\to 0} t_\sharp = \frac{\hbar\,\pi}{2\,\lambda}\,.$$

See right of Fig. 6 for the occupation probabilities $\mathcal{P}_{1,2}(t)$ in a case of a constant coupling strength $\lambda = 2.3$ and non-vanishing $\omega_c = 3$.

3.1.3. *Time-varying coupling $\lambda(t)$ and equal energy levels $\omega_c \equiv 0$.* Coming now to the time-dependent case (18) with $\omega_c \equiv 0$, the **site occupation probabilities** $\{\mathcal{P}_l(t)\}_{l=1}^2$ are given via (17) by

$$\mathcal{P}_1(t) = \cos^2\left(\frac{1}{\hbar}\int_0^t \lambda(s)\,ds\right)\,, \qquad \mathcal{P}_2(t) = \sin^2\left(\frac{1}{\hbar}\int_0^t \lambda(s)\,ds\right)\,. \tag{20}$$

The interpretation of these formulae is more delicate and to make concepts more concrete, we shall perform several numerical tests with specific $\lambda(t)$, in the aim to study the excitation transfer.

But before, let us start by making some observations. Firstly, recall that the coupling coefficient $\lambda(t)$ relies on the distance between the molecules of the chain (see expression (11)), and hence depends on the frequency ω_v of the underlying vibrational motion of the molecules. Now, a tricky coordination between the mechanical oscillation frequency ω_v and the Rabi frequency ω_R of the macroscopic oscillations may be beneficial for a quick and complete transfer of the excitation between site one and site two. To be more precise, take a look at formula (20) and remark for example that the period of the integrand $\lambda(s)$

is $T_v = \frac{2\pi}{\omega_v}$. If the vibrational motion is now synchronized such that one gets the relation $\frac{1}{\hbar}\int_0^{T_v} \lambda(s)\, ds = \pi$, then the probabilities $\{\mathcal{P}_l(t)\}_{l=1}^2$ are T_v-periodic with Rabi frequency $\omega_R := \omega_v$. For periods T_v which does not satisfy such a relation, the excitation transfer is no more periodic.

Let us go into more details and investigate the effect of the specific time-depending coupling strength $\lambda(t)$, given by

$$\lambda(t) := \frac{\tilde{\lambda}}{[d(t)/d_0]^3}\,, \quad d(t) := d_0\,[1 - 2a\,\sin(\omega_v\, t + \varphi)]\,, \quad a = 1/4\,,\ \ d_0 = \tilde{\lambda} = 1\,,\ \ \varphi = \pi/2\,, \tag{21}$$

on the occupation probabilities $\{\mathcal{P}_l(t)\}_{l=1}^2$, where we fixed for these tests $\hbar = 1$. In particular, we are interested in understanding the influence of the underlying vibrational frequency ω_v on the excitation transfer. Thus, to underline the dependence of λ and hence of its primitive on ω_v, let us denote

$$\Lambda(t, \omega_v) := \int_0^t \lambda_{\omega_v}(s)\, ds\,,$$

and study some of its properties in the next lemma.

Lemma 3.1. *The function*

$$\Lambda(t, \omega_v) = \int_0^t \frac{8}{[2 - \cos(\omega_v s)]^3}\, ds,$$

is strictly increasing in t, namely $\partial_t \Lambda(t, \omega_v) > 0$ for all ω_v, and satisfies moreover

$$\lim_{\omega_v \to +\infty} \Lambda(t, \omega_v) = \gamma\, t\,, \quad \gamma := \frac{1}{T_{\omega_v}} \int_0^{T_{\omega_v}} \frac{8}{[2 - \cos(\omega_v s)]^3}\, ds = \frac{4}{\sqrt{3}}\,, \quad \forall t > 0\,,$$

with $T_{\omega_v} := \frac{2\pi}{\omega_v}$. Thus, one has for the occupation probabilities

$$\mathcal{P}_2(t_\sharp) = \sin^2\left(\frac{1}{\hbar}\,\Lambda(t_\sharp, \omega_v)\right) = 1 \Longleftrightarrow \Lambda(t_\sharp^{(k)}, \omega_v) = \frac{(2k+1)\,\pi\,\hbar}{2}\,, \quad \forall k \in \mathbb{N}\,, \tag{22}$$

leading to a ω_v-dependent transfer time, which is oscillating in ω_v and satisfies (for $k = 1$)

$$t_\sharp(\omega_v) \to_{\omega_v \to \infty} \frac{\pi\,\hbar}{2\,\gamma} = \frac{\sqrt{3}}{8}\,\pi\,\hbar \approx 0.68\,.$$

Remark 3.2. *To vizualize the properties of this Lemma, we plotted on Figure 7 the phase-factor $\Lambda(t, \omega_v) := \int_0^t \lambda(s)\, ds$ as a function of time, and this for different ω_v-values, as well as the excitation transfer time $t_\sharp(\omega_v)$, for which $\mathcal{P}_2(t_\sharp(\omega_v)) = 1$.*

Proof. A simple change of variable yields (denoting $\omega_v = \omega$ for simplicity)

$$\Lambda(t, \omega) = \frac{1}{\omega} \int_0^{\omega t} \frac{8}{[2 - \cos(\tau)]^3}\, d\tau\,. \tag{23}$$

Assuming now that $\omega t \in [2k\pi, 2(k+1)\pi)$ for some $k \in \mathbb{N}$, permits to show that

$$\Lambda(t,\omega) \leq \frac{t}{2\pi}\int_0^{2\pi} \frac{8}{[2-\cos(\tau)]^3}\,d\tau + \frac{1}{\omega}\int_0^{2\pi} \frac{8}{[2-\cos(\tau)]^3}\,d\tau = \left(\frac{t}{2\pi}+\frac{1}{\omega}\right)\frac{8\pi}{\sqrt{3}}, \tag{24}$$

therefore

$$\lim_{\omega\to+\infty} \Lambda(t,\omega) \leq \frac{4t}{\sqrt{3}}.$$

In the same way

$$\Lambda(t,\omega) = \frac{k+1}{\omega}\int_0^{2(k+1)\pi} \frac{8}{[2-\cos(\tau)]^3}\,d\tau - \frac{1}{\omega}\int_{\omega t}^{2(k+1)\pi} \frac{8}{[2-\cos(\tau)]^3}\,d\tau \tag{25}$$

$$\geq \frac{t}{2\pi}\int_0^{2\pi} \frac{8}{[2-\cos(\tau)]^3}\,d\tau - \frac{1}{\omega}\int_0^{2\pi} \frac{8}{[2-\cos(\tau)]^3}\,d\tau = \left(\frac{t}{2\pi}-\frac{1}{\omega}\right)\frac{8\pi}{\sqrt{3}}, \tag{26}$$

hence

$$\lim_{\omega\to+\infty} \Lambda(t,\omega) = \frac{4t}{\sqrt{3}}.$$

□

But it is not only the transfer time which is of importance for the excitation transfer from site one towards site two. Indeed, another important aspect to be investigated is the time the transferred excitation spends on the second site. A tricky modulation of the coupling strength can elongate the effective time the excitation rests at site two, fact which enables this excitation to "jump" more rapidly to the next site (if the spin-chain is longer), and not to come back to the first site. This aspect, strictly related to the time-dependence of the coupling strength, will be discussed now in detail.

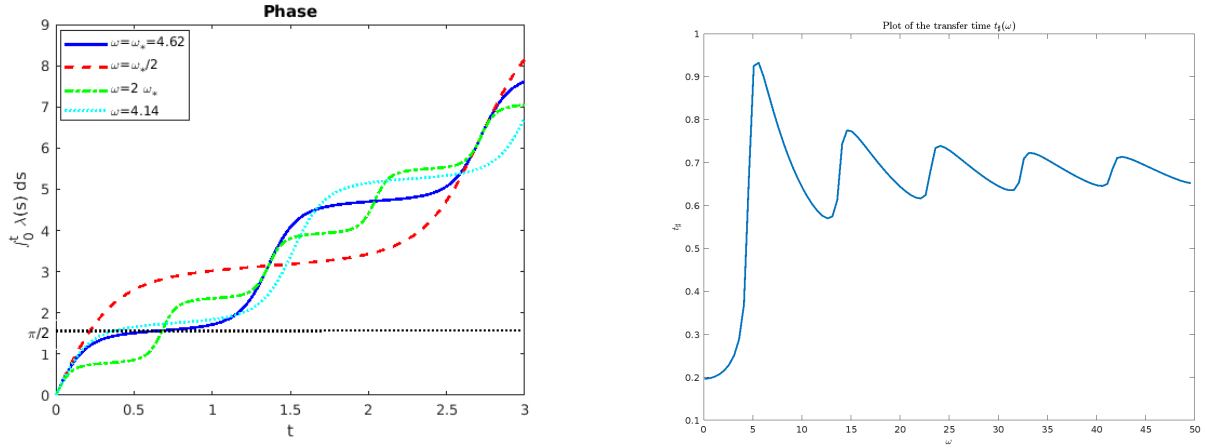

FIGURE 7. Left: Plot of the phase function $\Lambda(t,\omega_v) := \int_0^t \lambda(s)\,ds$. The plot for $\omega_v = \omega_\star$ corresponds to Fig. 8. Right: Plot of the transfer time $t_\sharp(\omega)$ with respect to the vibrational frequency ω_v.

In Figure 8 we plotted the shape of the coupling-strength $\lambda(t)$ given in (21) and the corresponding site occupation probabilities. Due to the mechanical oscillations of the underlying molecular structure, the coupling of the TLS exhibits narrow regions of strong interaction and larger regions of weaker interaction, this asymmetry is coming from the form of the dependence of $\lambda(t)$ upon the distance between the spins $d(t)$. What is expected is a faster excitation propagation between the sites whenever the coupling is stronger (meaning when two spins are closer to one another). A beating between the two spins is observed, similarly to the uniform coupling case of subsection 3.1.1, beating plotted on the right of Figure 8. But, contrary to the static coupling case, in the time-dependent configuration we observe the so-called *quick-transfer-and-locking-phenomenon* (term used in [2]). In other words, during the short time-interval of strong coupling, the excitation is quickly transferred from one site to the neighbouring one, whereas during the longer time-interval of weaker coupling, the excitation is locked on one site. One cannot visualize in this simple case with $N = 2$ spins the advantage of this *quick-transfer-and-locking-effect* on the excitation energy transfer, as for $N \leq 3$ the excitation is always completely transferred from the first to the last spin. However, the simple fact that, after being rapidly (and completely) transferred from spin 1 towards spin 2, the excitation remains locked at site 2 for some time, can be very advantageous. Indeed, the excitation has then a bigger probability to be carried over to a next site 3 (if the chain is longer) or to a sink, instead of being transferred back to site one. In this manner a transfer along the chain will be possible.

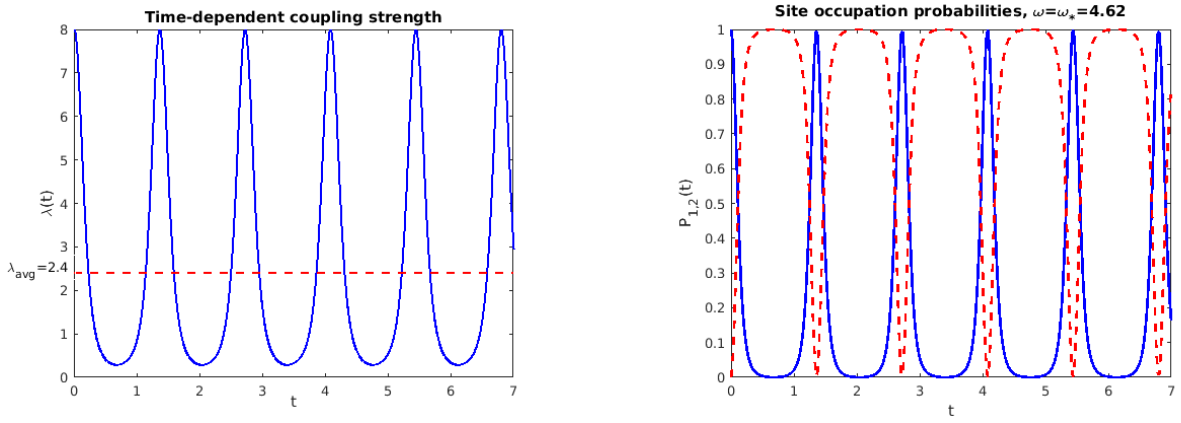

FIGURE 8. Left: Time evolution of $\lambda(t)$ for $\omega_\star = 4.62$. Right: Corresponding site occupation probabilities $\mathcal{P}_1(t)$ (full blue line) and $\mathcal{P}_2(t)$ (dashed red line).

In order to render this *quick-transfer-and-locking-phenomenon* efficient for the overall excitation transfer, a particular synchronization is required between the underlying classical oscillations and the quantum (Rabi) excitation oscillation, pictured for example by the formula of the occupation probability in the uniform energy-level case

$$\mathcal{P}_2(t) = \sin^2\left(\frac{1}{\hbar}\int_0^t \lambda(s)\,ds\right) = \sin^2\left(\frac{1}{\hbar}\Lambda(t,\omega_v)\right).$$

In this simplified case a synchronization arises when one requires that during half of the period of the mechanical oscillation $T_v/2$ the excitation is completely transferred from site one towards site two (see Fig. 8 for a better comprehension). This is achieved when asking for which $\omega_\star$ (if there is one) one has

$$\Lambda(T_v/2,\omega_\star)=\int_0^{T_v/2}\lambda_{\omega_\star}(t)\,dt=\frac{\pi}{2}\,\hbar\quad\text{leading to}\quad\mathcal{P}_2(T_v/2)=1\,.$$

This shall permit to obtain an optimal frequency $\omega_\star$ for which the excitation spends a maximal time on the second site. To compute this optimal frequency $\omega_\star$, we use a change of variable $\theta(s):=\lambda(s/\omega_\star)$ with $\lambda(t)$ given in (21), leading to

$$\frac{\pi}{2}\,\hbar=\int_0^{T_v/2}\lambda(t)\,dt=\frac{1}{\omega_\star}\int_0^{\pi}\theta(s)\,ds\quad\Rightarrow\quad\omega_\star=\frac{2}{\pi\,\hbar}\int_0^{\pi}\theta(s)\,ds\approx 4.62\,.$$

One can think it could be better to ask (as in [2]) that during a quarter of the mechanical oscillation period $T_v/4$ (during which the coupling is strong, see left of Fig. 8) the excitation is completely transferred from site one towards site two, namely to ask rather

$$\int_0^{T_v/4}\lambda(t)\,dt=\frac{\pi}{2}\,\hbar\quad\text{leading to}\quad\mathcal{P}_2(T_v/4)=1\quad\text{and}\quad\tilde{\omega}=\frac{2}{\pi\,\hbar}\int_0^{\pi/2}\theta(s)\,ds\approx 4.14\,.$$

The occupation probabilities corresponding to $\tilde{\omega}=4.14$ are plotted on Fig. 9. One remarks firstly that the curves are no more periodic, and secondly that the excitation arrives more rapidly at the last spin, however it remains there not as long as for $\omega_\star=4.62$.

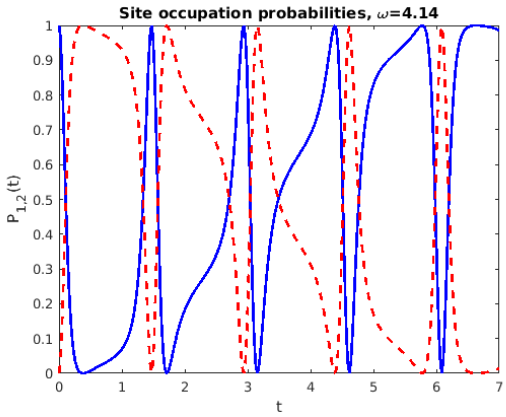

FIGURE 9. Time evolution of the site occupation probabilities $\mathcal{P}_1(t)$ (full blue line) and $\mathcal{P}_2(t)$ (dashed red line) for $\omega_v=\tilde{\omega}=4.14$.

On Figure 10 we plotted the site occupation probabilities for the two different vibrational frequencies $\omega_1:=\omega_\star/2$ and $\omega_2:=2\omega_\star$. When comparing these plots with the right plot of Fig. 8, which corresponds to the "optimal" frequency $\omega_\star$, we observe clearly a non-synchronization in these non-optimal frequencies ω_1,ω_2, which leads to a non-efficient excitation transfer within the spin-chain. Indeed, in this case one observes that the excitation, after being transferred to the second site (more or less rapidly), remains there only

for a short time and is transferred back to site 1. Thus, it would not have enough time to be transferred to a further spin, if the chain was longer.

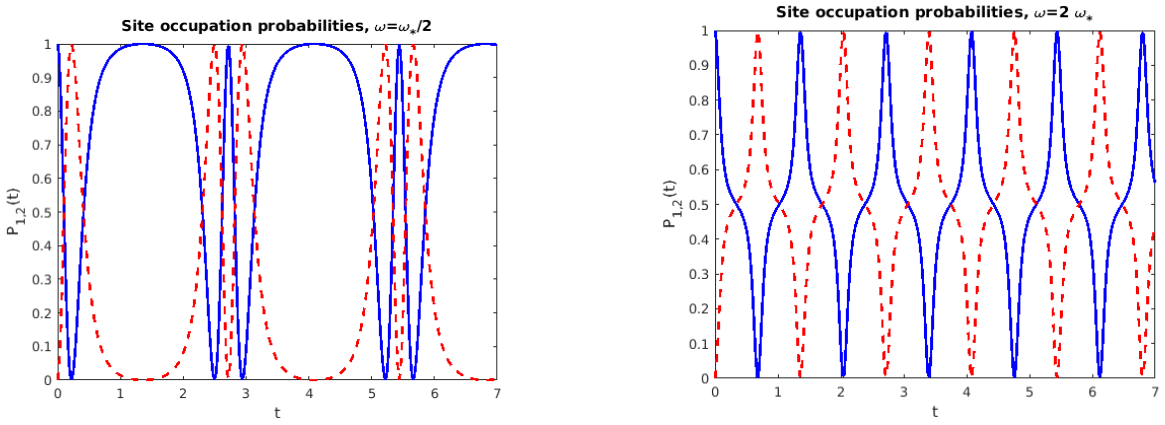

FIGURE 10. Site occupation probabilities $\mathcal{P}_{1,2}(t)$ for the two frequencies $\omega_1 = \omega_\star/2$ on the left and $\omega_2 = 2\omega_\star$ on the right.

To summarize, the observed effects of a modulation of the coupling strength $\lambda(t)$ (via the underlying mechanical oscillations) in the case of a chain of $N = 2$ spins, are:

- the transfer time from one end towards the other end of the chain is ω_v-dependent, however the excitation is always completely transferred;
- the time the excitation spans on the second site is also ω_v-dependent, with a maximum for a well-identified frequency $\omega_\star$.

3.2. **Driven model for $N = 7$ spins.** For longer spin-chains, as for example when considering the coupled pigments in a photosynthesis complex constituted of $N = 7$ sites, the excitation is no more completely transferred from the first to the last spin, and this due to the dispersion of the initial excitation over the whole spin-chain. What is now expected is an improvement of the transfer by manipulating the coupling strength, via the underlying mechanical oscillations of the molecular structure. In the former paper [23], one of the authors showed that for a particular static coupling configuration given by $\lambda_l := \lambda_0 \sqrt{l(N-l)}$ one obtains a perfect excitation transfer for all possible chain lengths, however this configuration is very sensitive to exteriour perturbations. In the present paper we follow a different idea, by introducing into the model the inevitable vibrational motion of the underlying molecular chain, and investigate its influence on the excitation energy transfer.

For long spin-chains with $N > 3$, one cannot do any more explicit computations, and we shall present in this section some numerical results for the driven sinusoidal model, with

$$d_l(t) := d_0 - \left[z_l^{(m)}(t) - z_{l+1}^{(m)}(t) \right] , \qquad z_l^{(m)}(t) := d_0\, a\, \sin\left(\frac{m\,\pi\, l}{N+1} \right) \sin(\omega_v\, t + \varphi) ,$$

$$\lambda_l(t) := \frac{\tilde{\lambda}_l}{[d_l(t)/d_0]^3}\,, \qquad \forall t > 0\,, \quad l = 1, \cdots, N-1\,,$$

where $m = 1, \cdots, N$ corresponds to the considered normal mode and

$$\varepsilon_l \equiv 0\,, \quad a \equiv 1/4\,, \;\; d_0 = \tilde{\lambda}_l \equiv 1\,, \;\; \varphi \equiv \pi/2\,, \;\; \hbar = 1\,, \quad \omega_v \in [2, 10]\,.$$

Choosing the mode $m = N$ means that we are considering again the breathing mode, as for the 2-spin chain, mode which can be associated with a human chain (bucket brigade for firefighting) transferring for example a water bucket from the reservoir towards the fire (see Fig. 11). This mode is the most appropriate one for an efficient excitation transfer, as shall be seen in the sequel, and this again if a certain synchronization is maintained between the underlying mechanical frequency and the quantum Rabi frequency.

FIGURE 11. Human chain representing the breathing mode of our spin-chain, inspiring a bucket-brigade device for an efficient excitation transfer (http://www.sylvesterdesign.com).

The numerical simulations are based on a resolution of the ODE system (14) via the Crank-Nicolson method. Let us discretize the time interval $[0, T_{fin}]$ in a homogeneous manner, with $\Delta t := T_{fin}/N_t$, $t_k := k\,\Delta t$, $k = 0, \cdots, N_t$ and where $N_t \in \mathbb{N}$ is the number of time intervals. Then the ODE system (14), written under the more general form

$$\left\{ \begin{array}{l} Z'(t) = A(t)\,Z(t)\,, \qquad t \in (0, T_{fin}] \\ Z(0) := Z_0 \in \mathbb{R}^N\,, \end{array} \right. , \qquad Z(t) := (\alpha_1(t), \cdots, \alpha_N(t))^{\mathbf{t}}\,,$$

is approximated by the following second-order A-stable Crank-Nicolson scheme

$$\left\{ \begin{array}{l} \left[Id - \dfrac{\Delta t}{2}\,A(t_{k+1})\right]\,Z^{k+1} = \left[Id + \dfrac{\Delta t}{2}\,A(t_k)\right]\,Z^k\,, \qquad \forall k = 0, \cdots, N_t - 1 \\ Z^0 \equiv Z_0\,. \end{array} \right.$$

In order to demonstrate how the presence of an underlying mechanical vibration can enhance the EET, we shall compare now the occupation probability at the last site $\mathcal{P}_7(t)$ for different coupling-strengths $\lambda(t)$, varying the frequency ω_v of the underlying oscillations,

as well as comparing the results with a static configuration (constant λ).

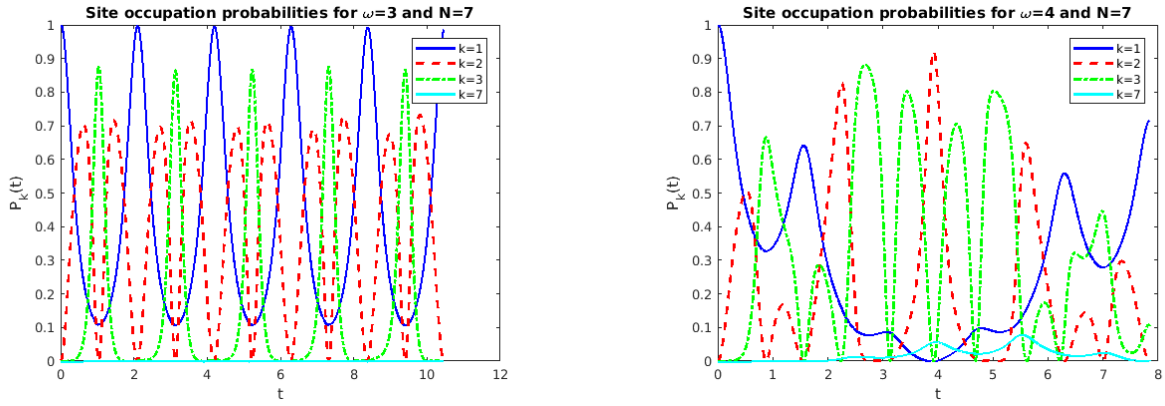

FIGURE 12. Site occupation probabilities $\mathcal{P}_k(t)$ for the two frequencies $\omega_v = 3$ and $\omega_v = 4$, and for $m = 7$, $N = 7$.

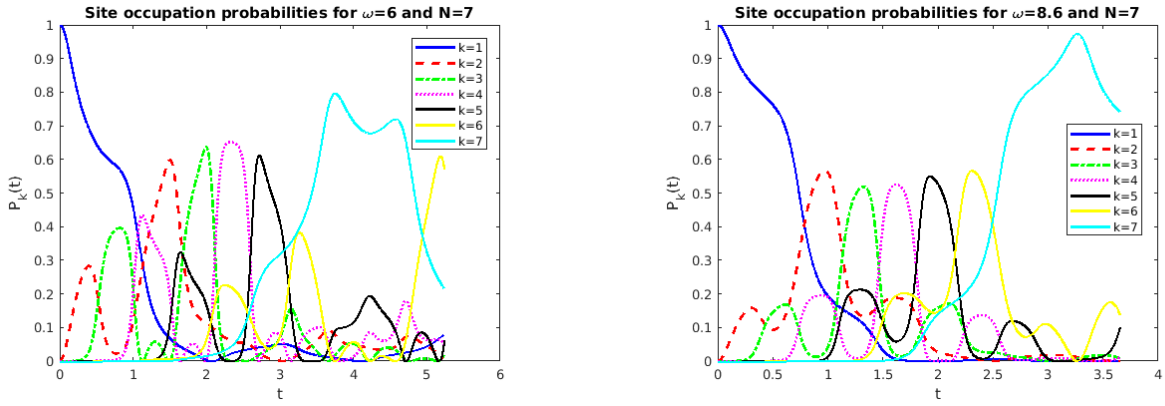

FIGURE 13. Site occupation probabilities $\mathcal{P}_k(t)$ for the two frequencies $\omega_v = 6$ and $\omega_v = 8.6$, and for $m = 7$, $N = 7$.

What can be observed from the series of Figures 12-14 is firstly that for a fixed mode ($m = 7$ for ex.) not all frequencies of the underlying motion are equally efficient for the excitation transfer from one end to the other end of the spin-chain. Indeed, for $\omega_v \equiv 3$ (left of Fig. 12) one remarks that the excitation is trapped between the first three spins, and does not reach the last spin. On Figures 12 (right) and 13 (left) we observe that the evolution of the excitation is that of a dispersed wave, which is not fully attaining the end point, but is somehow distributed over the whole chain. Finally it seems that starting from one particular frequency ($\omega_\star \approx 8.6$ in the breathing-case $m = 7$) the excitation is quasi fully transferred, frequency which corresponds again to a synchronization as for the chain of two spins (see right of Fig. 13 as well as Fig. 14).

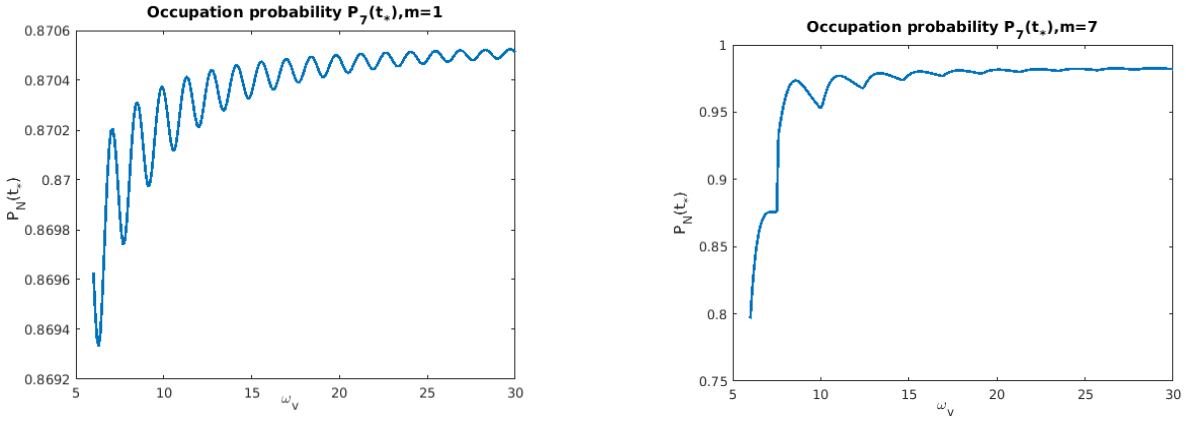

FIGURE 14. Site occupation probability $\mathcal{P}_7(t)$ as a function of the mech. frequency ω_v and for mode $m = 1$ (left) and $m = 7$ (right).

Secondly, we observe that there is a difference in the efficiency when comparing different modes of the mechanical oscillations, the "breathing" mode $m = 7$ being the most efficient one, as observed in Fig. 14, where for $m = 1$ one gets $\mathcal{P}_7(t_\sharp) \approx 0.87$ at $t_\sharp \approx 4.45$ and for $m = 7$, $\mathcal{P}_7(t_\sharp) \approx 0.983$ at $t_\sharp \approx 3.45$.
Finally a moving configuration surpasses the maximal static configuration (with $\lambda_{max} = \frac{1}{(1-2a)^3}$, $\mathcal{P}_7(t_\sharp) \approx 0.882$ at $t_\sharp \approx 0.56$) in the sense that the occupation probability $\mathcal{P}_7(t)$ attains values closer to one for the dynamical, synchronized configuration. Remark however that the fastest transfer, even if not complete, occurs for the maximal static coupling strength λ_{max}. Figure 15 presents a plot of the occupation probability for constant λ_{avg}, which is simply a time-dilatation or rescaling of the identical probabilities for λ_{max} and compares this plot with a driven configuration.

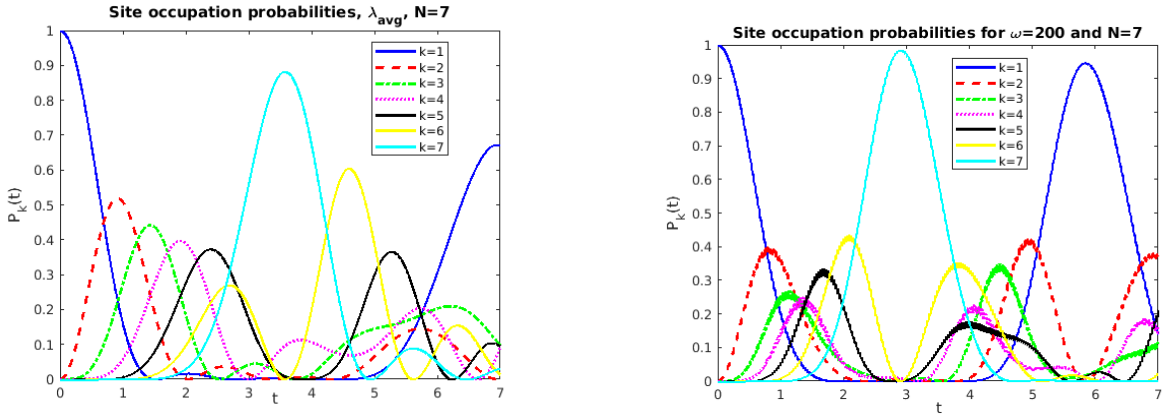

FIGURE 15. Site occupation probabilities $\mathcal{P}_k(t)$ for $N = 7$ and a constant coupling strength λ_{avg} (left) as well as a very high frequency $\omega_v = 200$ in the mode $m = 7$.

Some explanations for all these observed phenomena are the following:

- the quantum coherent excitation transfer allows to transfer the **entire** excitation (if there is a synchronization) from one site to the next one, fact which is not possible in a classical excitation transfer (via hopping);
- a modulation of the coupling strength can extend the effective time during which the excitation is localized close to the next site, as compared to the static configuration, and in this way permits a more efficient excitation transfer.

The fact that a well-orchestrated time-dependent coupling strength permits to enhance the excitation transfer as compared to a uniform coupling with strength λ_{max}, is a pure quantum mechanical effect. This provides a first evidence that biological systems (handling at room temperature) take advantage of non-trivial quantum mechanical effects in order to render its underlying processes efficient.

4. Conclusions and prospects

The aim of the present paper was to investigate how vibrations are involved in the excitation energy transfer (EET) of photosynthesis complexes, in particular the authors were interested in studying in more details the effect of the inevitable classical vibrations of a molecular chain on the quantum excitation energy transfer. In contrast to a previous work [23] where one of the authors used a fully quantum model, a hybrid quantum-classical model was used here in order to describe the EET. Furthermore the molecular motion is treated here as a coordinated dynamics, driving the excitation transfer, rather than a source of noise.

The here performed numerical simulations permitted to observe that, in order to be performant the pigment molecules in the photosynthesis complex are performing a concerted dynamics. Indeed, a well-arranged synchronization between the vibrational motion of the molecular chain and the wave-like quantum excitation transfer permits to boost the efficiency of the excitation transfer beyond the one of a static configuration. This mechanism of motion-induced excitation transfer enhancement is a veritable quantum signature of biological processes occurring in nature.

What is interesting to be observed is that the coupling strength $\lambda(t)$ enters into the computation of the site occupation probability via an integration. Thus, small perturbations of these coupling coefficients, due for example to environmental noise, will probably not be so dramatic, as compared to a static coupling case. This remains to be investigated in a future work.

Another question which remains to be studied in subsequent works is to generalize this model or concepts to more general, multi-dimensional settings, working on quantum networks. The presence of multiple paths between the photon-acceptor and the photon-receiver, which could coherently interfere with each other, could reinforce even more the excitation energy transfer.

Acknowledgments. The author would like to acknowledge support from the CNRS-IEA project N^o 295470 *NASOQUAD* (Numerical and Analytical Study Of QUAntum Decoherence, 2020-2022).

References

[1] D. Abbott, P.C.W. Davies, A.K. Pati, *Quantum aspects of life*, Imperial College Press 2008.
[2] A. Asadian, M. Tiersch, G.G. Guerreschi, J. Cai, S. Popescu, H.J. Briegel *Motional effects on the efficiency of excitation transfer*, New J. Phys. **12** (2010), 075019.
[3] C. H. Bennett, D. P. Di Vincenzo, *Quantum information and computation* Nature **404** (2000), 247–255.
[4] R.E. Blankenship *Molecular Mechanisms of Photosynthesis*, Blackwell Science Ltd Oxford, 2002.
[5] Ph. Blanchard, D. Giulini, E. Joos, C. Kiefer, J. Kupsch, I.-O. Stamatescu, H.D. Zeh, *Decoherence and the Appearance of a Classical World in Quantum Theory*, Springer, 1996.
[6] H.-P. Breuer, F. Petruccione, *The Theory of Open Quantum Systems*, Oxford University Press, Oxford, 2007.
[7] J. Cai, S. Popescu, H.J. Briegel *Dynamic entanglement in oscillating molecules and potential biological implications*, Phys. Rev. E **82** (2010), 021921.
[8] H.B. Chen, C. Gneiting, P.Y. Lo, Y.N. Chen, F. Nori *Simulating Open Quantum Systems with Hamiltonian Ensembles and the Nonclassicality of the Dynamics*, Phys. Rev. Lett. **120** (2018), 030403.
[9] M. Christandl, N. Datta, T.C. Dorlas, A. Ekert, A. Kay, A.J. Landahl *Perfect transfer of arbitrary states in quantum spin networks*, Phys. Rev. A **71** (2005), 032312.
[10] A.C.C. Coolen *A Beginner's Guide to the Mathematics of Neural Networks*, Landau L.J., Taylor J.G. (eds) Concepts for Neural Networks. Perspectives in Neural Computing. Springer, London, 1998.
[11] M. Correggi, M.Falconi, M. Fantechi, M. Merkli *Quasi-classical Limit of a Spin Coupled to a Reservoir*, Quantum **8** (2024), 1561–1591.
[12] D. Crow, R. Joynt *Classical simulation of quatum dephasing and depolarizing noise*, Phys. Rev. A **89** (2014), 042123.
[13] G.S. Engel et al., *Evidence for wavelike energy transfer through quantum coherence in photosynthetic systems*, Nature **446** (2007), 782–786.
[14] M. P. Estarellas, *Spin Chain Systems for quantum computing and quantum information applications*, PhD thesis, University of York, 2018.
[15] B. Gu, I. Franco *When can quantum decoherence be mimicked by classical noise?*, J. Chem. Phys. **151** (2019), 014109.
[16] G.G. Guerreschi, J. Cai, S. Popescu, H.J. Briegel *Persistent dynamic entanglement from classical motion: How bio-molecular machines can generate non-trivial quantum states*, New Journal of Physics **14** (2012), 053043.
[17] A. Ishizaki, G. R. Fleming, *Quantum Coherence in Photosynthetic Light Harvesting*, Annual Review of Condensed Matter Physics **3** (2012), 333–361.
[18] E. Joos, H.-D. Zeh, *The Emergence of Classical Properties Through Interaction with the Environment*, Z. Phys. B59, (1985) 223–243.
[19] N. Lambert et al., *Quantum biology*, Nature Physics **9** (2013), 10–18.
[20] H. Lee, Y.C. Cheng, G.R. Fleming, *Coherence dynamics in photosynthesis: protein protection of excitonic coherence*, Science **316** (2007), 1462–1465.
[21] S. Lloyd, *Quantum coherence in biological systems*, J. Phys.: Conf. Ser. **302** (2011), 012037.
[22] R. Kosloff *Quantum thermodynamics and open-systems modeling*, J. Chem. Phys. **150** (2019), 204105.
[23] C. Negulescu, *Decoherence rhapsody in the photosynthesis process*, CMS (Communications in Mathematical Sciences) **19** (2021), no. 4, 947–975.
[24] M. Schlosshauer, *Decoherence and the Quantum-To-Classical Transition*, Springer-Verlag (2007).
[25] G.D. Scholes, *Long-range resonance energy transfer in molecular systems*, Ann. Rev. Phys. Chem. **54** (2003), 57–87.

[26] G.D. Scholes, G.R. Fleming, *On the Mechanism of Light Harvesting in Photosynthetic Purple Bacteria: B800 to B850 Energy Transfer*, J. Phys. Chem. B **104** (2000), 1854–1868.

Università degli Studi di Napoli Federico II, Dipartimento di Matematica e Applicazioni "Renato Caccioppoli", Via Cintia, Monte S. Angelo, 80126, Napoli, Italy
Email address: raffaele.carlone@unina.it

Università degli Studi di Napoli Federico II, Dipartimento di Matematica e Applicazioni "Renato Caccioppoli", Via Cintia, Monte S. Angelo, 80126, Napoli, Italy
Email address: ilenia.digiorgio@unina.it

Université de Toulouse & CNRS, UPS, Institut de Mathématiques de Toulouse UMR 5219, F-31062 Toulouse, France.
Email address: claudia.negulescu@math.univ-toulouse.fr